Fuel 268 (2020) 117365

Contents lists available at ScienceDirect

Fuel

journal homepage: www.elsevier.com/locate/fuel

Full Length Article

TG-FTIR for kinetic evaluation and evolved gas analysis of cellulose with different structures

Fei-xiang Xu[a,1], Xu Zhang[a,1], Fan Zhang[b,1], Li-qun Jiang[a,*], Zeng-li Zhao[a], Hai-bin Li[a]

[a] Key Laboratory of Renewable Energy, Guangdong Key Laboratory of New and Renewable Energy Research and Development, Chinese Academy of Sciences, Guangzhou Institute of Energy Conversion, Guangzhou 510640, China

[b] CAS Key Laboratory of Tropical Plant Resources and Sustainable Use, Xishuangbanna Tropical Botanical Garden, Chinese Academy of Sciences, Menglun, Mengla, Yunnan 666303, China

ARTICLE INFO

Keywords:
Cellulose
Thermogravimetric analysis
Kinetics
TG-FTIR

ABSTRACT

In this study, the effect of structural characteristics of cellulose on its pyrolysis behavior was investigated. The structure of crystalline cellulose was altered by ball milling (BM) pretreatment, resulting in decreases in crystallinity and degree of polymerization. The initial pyrolysis temperature of BM-cellulose decreased, as well as the temperature at which maximum weight loss rate was achieved. Moreover, BM-cellulose was observed to produce more solid residue. The pyrolysis process was fitted by n-order reaction model. The global activation energy of Un-treated cellulose (228.3–270.6 kJ/mol) was higher than that of BM-cellulose (166.8–187.0 kJ/mol). TG-FTIR experiment showed that BM-cellulose yielded more CO_2 and H_2O than Un-treated cellulose. This research provided a comprehensive analysis of the effects of structural characteristics of cellulose on the pyrolysis behavior of cellulose.

1. Introduction

With the increasing population, rising energy demand, and developing urbanization, traditional fossil fuels are faced with a threat of depletion, drawing a wide range of concerns from human society [1]. Moreover, the overuse of fossil fuels also causes lots of environmental problems. In order to transform the present situation, a renewable and clean alternative energy is needed. As one of the most widely distributed renewable resources in nature, biomass energy has various applications, such as producing chemicals and power (heat and electricity), which is considered as a promising substitution for fossil fuels [2]. Lignocellulose is the most abundant form of renewable natural resources and always exists as residue of agriculture and forestry. Lignocellulosic biomass can be utilized for gaseous fuels, bioethanol, and value-added chemicals production via biochemical and thermochemical conversion [3]. There are three main components of lignocellulose, cellulose, hemicellulose and lignin, among which cellulose has the highest proportion [4]. Cellulose is a polysaccharide composed of cellobiose which is linked with each other by β-1,4-glycosidic bond to form a long molecular chain [5]. The degree of polymerization (DP) of cellulose refers to the number of D-glucose groups in the macromolecular chain of cellulose, which indicates the length of the cellulose chain. Cellulose can be divided into crystalline cellulose and amorphous cellulose [6]. Cellulose molecular chains are aligned and relied on hydrogen bonding at the side chains of the cellulose to form a crystalline lattice in the crystalline area. In contrast, the amorphous cellulose molecules are disorderly arranged and loose, and no crystalline lattice is formed. Cellulose molecules are composed of regular crystal region and irregular amorphous region. There is no obvious boundary within the crystalline and amorphous regions, thus a gradual transition phenomenon is exhibited.

Pyrolysis is a process of thermochemical conversion. It can continuously convert low-energy-density biomass into high-energy-density gas, liquid, and solid products at a low cost. The main pyrolytic products of cellulose are anhydro-sugars and its derivatives, furan compounds, small molecule chain compounds, coke and non-condensable gases [7]. Lignocellulose with different compositions and structures exhibits large differences on products distribution [8–10]. In terms of cellulose, there is still controversy about whether the physical structural characteristics of cellulose has an impact on the distribution of pyrolysis products. Some scholars hold that the crystallinity and DP of cellulose had nothing to do with the distribution of cellulose pyrolysis products [11,12]. Nevertheless, there is also some literature indicating that the structural characteristics of cellulose have a considerable

* Corresponding author.
E-mail address: lqjiang@ms.giec.ac.cn (L.-q. Jiang).
[1] These authors contributed equally to this work.

https://doi.org/10.1016/j.fuel.2020.117365
Received 2 December 2019; Received in revised form 6 February 2020; Accepted 8 February 2020
Available online 21 February 2020
0016-2361/

influence on its pyrolysis behavior, however, there is insufficient experimental data to demonstrate it. In order to gain a deeper understanding of the effects of the structure of cellulose on its pyrolysis, more research is necessary [13].

Thermogravimetric analysis (TGA) is a thermal analysis technique that estimates the relationship between mass and temperature, which is generally used to express the thermal stability and composition of samples. Combined thermogravimetric analysis with Fourier transform infrared spectrometry (TG-FTIR) can be used to identify gaseous species during pyrolysis and assess the distribution of gaseous products [14–16]. This method provides the convenient of real-time measurement while not destroying multiple gas phase compounds in a complex mixture. Therefore, TG-FTIR technology is applied to study the thermal behavior of various materials during pyrolysis and combustion [17–19]. An important aspect of studying cellulose pyrolysis is the thermogravimetric curve and kinetic analysis. The graph obtained by TG can be effectively employed to understand the dynamic characteristics of the pyrolysis process, which plays a considerable role in optimizing pyrolysis process. The effect of the heating rate and pyrolysis temperature of the raw materials on the pyrolysis can be obtained by thermogravimetric and kinetic analysis [20]. These methods take a global perspective and seek an apparent dynamic model reflecting the whole pyrolysis process of cellulose. According to the reaction route and steps, the cellulose pyrolysis reaction model can be divided into three categories: one-step global reaction model, two-step reaction model and multi-step comprehensive reaction model. The one-step global reaction model was commonly used in the early stage of research, and it is believed that the cellulose pyrolysis reaction is one step in place, and the pyrolysis of cellulose at high temperatures produces coke and volatile matter. The two-step reaction model can also be divided into two-step competition and two-step continuous reaction model. The two-step reaction model takes into account the secondary decomposition in the process of cellulose pyrolysis, and considers that the pyrolysis process is carried out in two steps, which is more in line with the reality of cellulose pyrolysis than the one-step global reaction [21]. Compared with the one-step reaction model and the two-step reaction model, the multi-step comprehensive reaction model is the most developed model at present, which is conducive to the accurate solution of kinetic parameters.

Ball milling (BM) is a fascinating choice to change the structure of cellulose. The BM-pretreatment applies some high-speed rotating steel balls to grind the cellulose into a powder, thereby destroying the crystal structure and DP of cellulose. In this study, to explore the influence of structural characteristics of cellulose on the pyrolytic product distribution and formation mechanism, BM-pretreatment was applied to alter the structure of cellulose. TG-FTIR was applied to analyze the difference in pyrolysis behavior of cellulose with different structures, and the parameters of the kinetic model were also obtained from the TG curve. The n-order reaction model was used to calculate the activation energy required for cellulose pyrolysis, which reflected the influence of the structural characteristics of cellulose on its physical and chemical properties. This study provided experimental data to elaborate the effect of the structure of cellulose on the pyrolysis behavior, thereby providing useful information to improve the selectivity of the product.

2. Materials and methods

2.1. Ball milling pretreatment

Microcrystalline cellulose (Avicel® PH-101) was produced by Sigma-Aldrich. Ball milling pretreatment was performed in a planetary ball mill. The planetary ball mill had four 50 mL ball mill tanks. Cellulose (8 g) was divided into four ball milling tanks on average. Each ball mill tank was placed with the same number of ball mill beads. The rotation speed was set at 300 rpm for 6 h. At the beginning of the experiment, the rotation of the turntable caused the ball mill tank to revolve, the ball mill tank rotated at the same time, causing the ball mill beads rotated at high speed, and a severe collision occurred in the tank to fully grind cellulose. The pretreated sample was named as BM-cellulose.

2.2. Elemental analysis and structural characterization

Alkali and alkaline earth metals (AAEMs) analysis was conducted on an Inductively Coupled Plasma Optical Emission Spectrometry (ICP-OES, OPTIMA 8000DV, PerkinElmer, USA). Microscopic surface morphology of cellulose was obtained from a Scanning Electron Microscope (SEM, S-4800, Hitachi, Japan) system. Specific surface area of cellulose samples was determined by Brunauer-Emmett-Teller (BET) method. For DP analysis, cellulose was transformed into the phenyl carbamate derivative and then analyzed by Gel Permeation Chromatography (GPC). X-ray diffraction (XRD) analysis was carried out in an X-ray diffractometer (X'Pert PRO MPD, PANalytical B.V., the Netherlands) and the crystallinity index (CrI) of the samples was calculated according to previous research [22]. FTIR analysis was conducted on BRUKER TENSOR 27 (Germany).

2.3. TG-FTIR

The TG-FTIR experiment was carried out in a TG system (Q50, TA, USA) coupled with an FTIR spectrometer (Nicolet 6700, Thermo, USA). For each experiment, the sample was heated from 30 °C to 750 °C at a heating rate of 10, 20, 40 and 80 °C/min, respectively, and kept at 750 °C for 30 min. The flow rate of nitrogen used as the carrier gas was kept at 40 mL/min. The comprehensive pyrolysis index (P) was generally applied to evaluate the degree of pyrolysis reaction. The formula was shown below.

$$P = \frac{D_{\max}}{T_{\max}(T_t - T_i)} \tag{1}$$

where D_{max} refers to the mass loss according to the DTG peak, T_{max}, T_t and T_i refer to the temperature according to the DTG peak, the terminal temperature of main mass loss zone with the weight loss at 80% and the initial temperature of main mass loss zone with the weight loss at 5%, respectively.

The volatiles of TG process were sent to the FTIR spectrometer with a transfer line which was heated at a constant temperature of 300 °C. The products were detected by FTIR measurements and their spectra was recorded from 600 to 4000 cm^{-1}.

2.4. Kinetic analysis

The pyrolysis of cellulosic samples was assumed as n-order chemical reaction which was described by n-order reaction model. The conversion rate of samples during pyrolysis was defined as follows:

$$\alpha = \frac{m_0 - m}{m_0 - m_\infty} \tag{2}$$

where m_0 was the initial sample mass, %; m was the sample mass at a special time, %; m_∞ was the final sample mass, %.

According to the Arrhenius law, reaction rate of solid phase could be expressed as the following equation:

$$\frac{d\alpha}{dt} = A\exp\left(-\frac{E}{RT}\right)f(\alpha) \tag{3}$$

where R was general gas constant, 8.314 J/(mol·K); A was the pre-exponential factor, E was the activation energy, $f(\alpha)$ was the kinetic model function.

The relationship between the heating rate and temperature in the linear heating program was $\beta = dT/dt$. Then the kinetic equation was turned into Eq. (4):

$$\frac{d\alpha}{dT} = \left(\frac{A}{\beta}\right)\exp\left(-\frac{E}{RT}\right)f(\alpha) \tag{4}$$

The most common form of kinetic model function was Eq. (5):

$$f(\alpha) = (1-\alpha)^n \tag{5}$$

where n was the reaction order.

Substituting Eq. (5) into Eq. (4), then taking the logarithm of Eq. (4) and making the difference, Eq. (6) was obtained:

$$\frac{\Delta \ln(\frac{d\alpha}{dT})}{\Delta \ln(1-\alpha)} = -\frac{E}{R}\left[\frac{\Delta(\frac{1}{T})}{\Delta \ln(1-\alpha)}\right] + n \tag{6}$$

The terms in the brackets of right side and left side of the Eq. (6) were linear. The activation energy E and the reaction order n were determined by the slope and intercept of the fitted straight. Pre-exponential factor A was calculated by substituting values of E and n into Eqs. (4) and (5).

The existence of the kinetic compensation effect was the result of the exponential form of the rate constant of Arrhenius law. The kinetic compensation effect could be expressed as Eq. (7):

$$\ln A_{app} = E_{app}/RT_{iso} + \ln k_{iso} \tag{7}$$

where T_{iso} and k_{iso} were isokinetic temperature and isokinetic rate constant, respectively. The kinetic compensation effect was regarded as the projection of the internal relations of lnA, E and T on the ln$A$-E plane. The kinetic compensation effects were divided into two categories according to the existence condition: one was that different results were obtained by using the same experimental conditions in the same system, and the other was that an incorrect dynamic mechanism function was used by the single TG curve.

3. Results and discussions

3.1. Elemental analysis and structural characterization

The ICP results of different cellulose samples are shown in Table 1. After BM-pretreatment, significant changes weren't observed in the content of AAEMs and the percentage difference was within ± 0.2%. However, there was a significant difference in the DP between the Un-treated cellulose and BM-sample. Thereby, the catalytic effect of AAEMs could be ignored. The surface morphology of Un-treated cellulose was relatively compact and exhibited an irregular elongated shape. Compared with Un-treated sample, BM-cellulose was pulverized into pellets from long pieces, emerging many fine crystal powders (Fig. 1), and the difference in appearance between the powders became small. This irregular loose morphology might facilitate the escape of volatiles from the cellulose pyrolysis product. The specific surface area, DP and CrI of Un-treated cellulose were 0.9 m^2/g, 260 and 89.9% respectively (Table 1). After BM-pretreatment, the large cellulose particles were changed into small particles and the specific surface area was increased, which was favorable for heat and mass transfer in the pyrolysis process. The cellulosic granules were grinded into smaller size with 57.7% decline in DP. The CrI of BM-cellulose was reduced by 61.0%, indicating that the crystalline structure was greatly destructed by mechanical force.

Table 1
The structure parameters of Un-treated cellulose and BM-cellulose.

Samples	Structure parameters			AAEMs (ppm)			
	Specific surface area (m^2/g)	DP	CrI (%)	K	Na	Ca	Mg
Un-treated cellulose	0.9	260	89.9	1.6	3.8	4.7	0.3
BM-cellulose	1.0	110	35.1	1.3	3.9	4.4	0.2

FTIR could be applied to detect functional groups in different cellulose samples [23]. The positions of the infrared characteristic peaks of the two groups of samples were basically the same, and the peak shapes were also very similar. The main difference was the intensity of peaks, indicating that the BM-pretreatment did not cause the cellulose to generate new functional groups. According to the Lambert-Beer law, the transmittance of the characteristic absorption peak was linearly dependent on the relative concentration of the functional groups [19]. The transmittance of the characteristic absorption peak of the BM-cellulose was larger, indicating that the BM-cellulose was detected with more functional groups with the same amount of sample. This might be explained that the BM-pretreatment increased the specific surface area of the cellulose, exposing more functional groups to the surface. As shown in Fig. 2, most of peaks mainly occurred at 2900–3600 cm^{-1} and 897–1500 cm^{-1}. Two different types of cellulose exhibited strong OH transmission peaks at 3413 cm^{-1} and fluctuated at 2900 cm^{-1} because of the stretching vibrations of CH group. The 1368 cm^{-1} was attributed to the bending vibrations of CH group. The reason for the transmission peak in the range of 1060–1150 cm^{-1} was that the C-O-C had symmetric stretching vibrations and asymmetric stretching vibrations. When below the 1000 cm^{-1}, the shear bending vibrations and the respiratory vibrations of saccharide ring led to the appearance of some transmission peaks.

3.2. Thermogravimetric analysis

TG and DTG curves of cellulosic samples at different heating rates are showed in Fig. 3. The thermal degradation of cellulosic samples had only one evident weight loss area caught the main weight loss zone. As marked in Fig. 3 (10 °C/min), T_i and T_t were the initial and terminal temperature of main weight loss zone respectively. The pyrolysis process of sample could be divided into three phases. The initial phase was from the beginning of heating to T_i when the cellulose was dehydrated. Then a slight weight loss stage and a glass transition occurred to form dehydrated cellulose. The yield of volatiles was extremely low at this stage. The second stage was the main weight loss stage from T_i to T_t when the thermal reaction became intensive, yielding a large amount of volatiles. When the temperature reached T_{max}, the weight loss rate reached to the peak value D_{max}. Then the DTG curves began to go down with increasing temperature and the thermogravimetric process was near the end at T_t. The third stage was carbonization stage where the TG and DTG curves were almost flat and the residue formation from the second stage was carbonized.

The thermal characteristic parameters are presented in Table 2. In most case, the T_i and T_{max} of BM-cellulose were lower than those of Un-treated cellulose at different heating rates. Excluding the influence of material thermal resistance, the sample with lower crystallinity decomposed at a lower temperature and it could be ascribed to the destruction of cellulose structure by BM-pretreatment. Un-treated cellulose decomposed at higher temperature range due to long-chain structure of crystalline cellulose, exhibiting good thermal stability [24]. However, after pretreatment, the long-chain structure of cellulose was destroyed resulting in the decrease of cellulose stability. For crystalline cellulose, the DTG peak shifted to higher temperatures with decrease in peak mass loss rate and no change was observed in shape as heating rate increased. This phenomenon was known as “thermal hysteresis” [25]. The decrease in peak mass loss rate might be attributed to the considerable difference of temperature between the surface and interior of the cellulosic particle at a high heating rate. The peak weight loss of crystalline and amorphous cellulose was similar at the identical heating rate, indicating that semblable volatiles released during this process.

The final residue was considered as coke of which weight fraction was marked as M_r. The M_r of Un-treated cellulose was lower than that of BM-cellulose. The results showed that BM-cellulose yielded more solid residues than Un-treated cellulose, which could be attributed to the

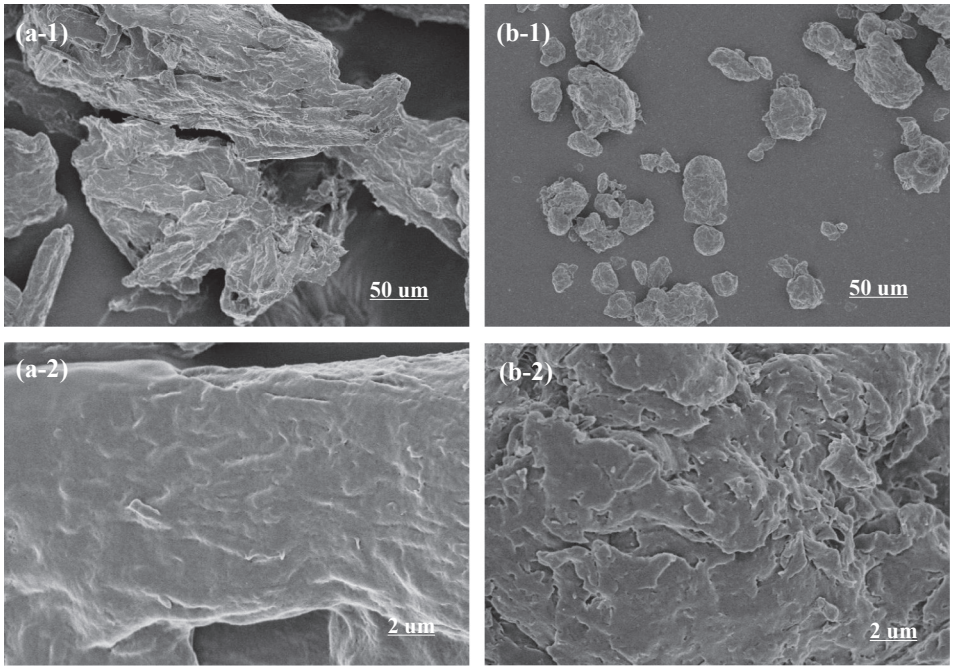

Fig. 1. Surface structure characteristics of Un-treated cellulose (a) and BM-cellulose (b).

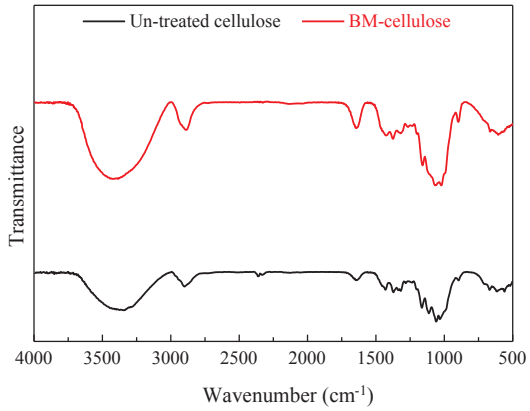

Fig. 2. FTIR spectra of Un-treated cellulose and BM-cellulose.

decrease of DP and CrI. Low weight and length of cellulosic molecules generated higher yields of char, and the reduction of DP could induce the formation of char [11,26]. The decrease of crystallinity caused the amorphous cellulose to easily change from a solid state to a molten state at a high temperature, thereby forming a fluffy porous coke [27]. The comprehensive pyrolysis index P was used to evaluate the severity of the main thermal degradation process [28]. The higher the comprehensive index P was, the more violent the cellulosic samples decomposed. The comprehensive pyrolysis indexes of Un-treated cellulose and BM-cellulose at 10 °C/min were 16.4 and 11.8%/°C^2 respectively. The cellulose with higher crystallinity had higher P value, representing the thermal decomposition was more violent and explosive. A similar conclusion was also obtained from the results at other heating rates.

3.3. Kinetic analysis

The activation energy (E), reaction order (n), pre-exponential factor (A) and coefficients of determination (R^2) of the two samples at different heating rates are listed in Table 3. The fitting straight-lines of Un-treated cellulose and BM-cellulose based on n-order reaction model are shown in Fig. 4. As shown in Fig. 4, the scatter points almost distributed on the fitting straight-line, which meant that the predicted results of the kinetic model accorded well with the experimental results, exhibiting a higher R^2 value. The closer the R^2 was to 1, the better the fitting effect was. The R^2 of crystalline cellulose and amorphous cellulose was totally evaluated as around 0.99, indicating that the pyrolysis reaction rate of Un-treated and BM-cellulose could be well simulated by n-order reaction model.

The reaction order, activation energy and pre-exponential factor of BM-cellulose were obviously reduced. The activation energy range of Un-treated cellulose was a range of 228.3–270.6 kJ/mol, as for BM-cellulose, the activation energy was 166.8–187.0 kJ/mol. Since the global activation energy E corresponded to the thermal stability of the sample, while Un-treated cellulose had a larger E, indicating that more energy was required to decompose. The major reason was that the chain length of cellulose was reduced and the crystalline structure was destroyed by BM-pretreatment. The surface of Un-treated sample showed a compact block structure with the crystallinity of 89.9%, indicating that the molecular structure of the microcrystalline cellulose was highly ordered and the interactions between the molecules were built by van der Waals force, and finally resulting in the high heat resistance at the initial stage of pyrolysis [2]. The crystallinity of BM-cellulose was low (35.1%), and the molecular unit structure was relatively loose and disordered, leading to the lower thermal stability and global activation energy. The pre-exponential factor of BM-cellulose (10^{14} s^{-1}) showed a significant decrease compared with that of Un-treated cellulose (10^{20} s^{-1}), which eventually led to a decrease in reaction order of BM-cellulose (0.2–0.5), indicating that the crystalline cellulose had more reactivity in a short time [29]. In the n-order reaction model, there was a close correlation between the kinetic parameters (the reaction order and the pre-exponential factor) and the reaction intensity during pyrolysis. There was a strong interaction force between the Un-treated cellulose molecules due to van der Waals force. When the temperature rose to a certain extent, a relatively concentrated structural collapse occurred prior to a large-scale decomposition reaction occurring rapidly. However, the molecular unit of BM-cellulose was relatively loose and disordered, causing the weak interaction force, which reduced the pyrolysis reactivity of cellulose.

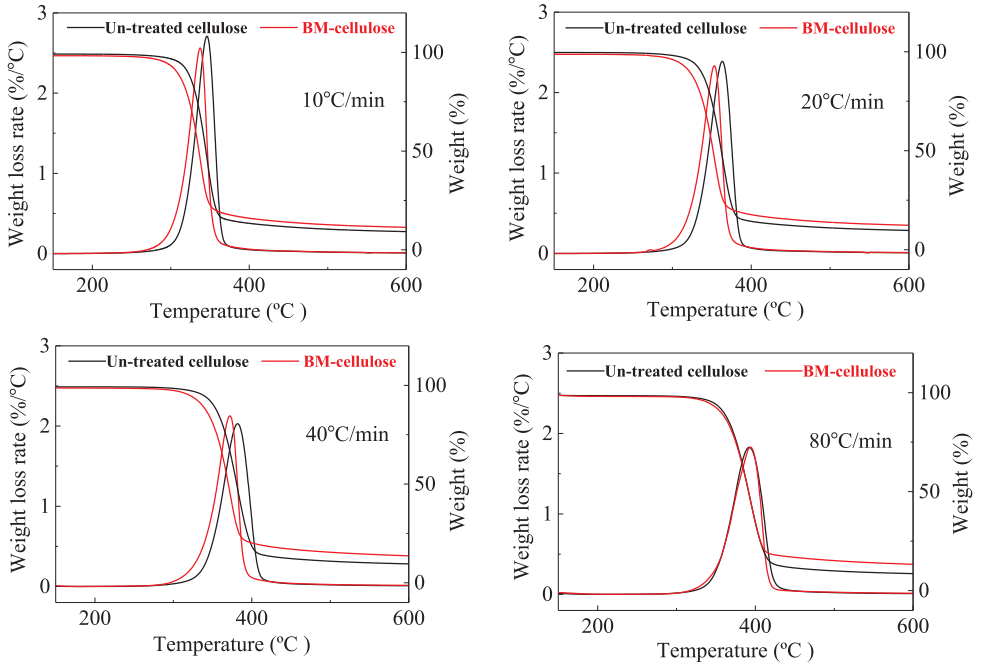

Fig. 3. TG and DTG curves at different heating rates.

3.4. FTIR analysis of pyrolysis products from cellulose

The gaseous products of TG were examined by FTIR in order to have a better understanding for the pyrolysis mechanism of cellulose with different structures. According to the Lambert-Beer Law, the concentration of release products was linearly reflected on the intensity of absorbance at specific wavenumber. Thus, the IR peak heights represented the generated concentration of gaseous products. FTIR experiment was applied for real-time detection of cellulose pyrolysis to obtain three-dimensional spectrogram (Fig. 5). The three-dimensional coordinates referred to time, wavenumber and absorbance, respectively. It could be clearly observed that the cellulose first pyrolyzed to produce water at the beginning of the experiment, prior to a large number of volatiles, then gradually decreased, but the infrared spectrum maintained a certain intensity peak until the final stage. Both crystalline and amorphous cellulose pyrolysis both produced a large proportion of CO_2, C=O (ketone, aldehydes, carboxylic acid, esters) and C=C (alkene, aromatics), with a small amount of H_2O and CH_4 evolving (Fig. 6). Most of the gaseous products released intensively at a small range, which was related to the main weight loss zone [30]. As the heating rate increased, the weight loss peak occurred earlier compared with the absorbance peak because of the slight time difference between TG and FTIR instrument.

The maximal absorbance intensity of gaseous products, functional groups and corresponding temperature are showed in Table 4. The FTIR curves of functional groups or products at maximal absorbance intensities (CO_2 2357 cm^{-1}, H_2O 3566 cm^{-1}, CH_4 2810 cm^{-1}, C=O 1746 cm^{-1}, C=C 1508 cm^{-1}, CO 2181 cm^{-1}, C-O-C/C-C 1061 cm^{-1}) are presented in Fig. 6. The IR peak of CO_2 was the highest among all products during the pyrolysis of cellulose with crystalline and amorphous structures at different heating rates except for the pyrolysis of Un-treated cellulose at 10 and 80 °C/min. It could be obviously observed that BM-cellulose yielded more CO_2 and H_2O than crystalline cellulose. The formation of CO_2 during the cellulose pyrolysis was mainly attributed to the degradation of dehydro-cellulose at the early stage and the reforming of C=O and COOH at high temperature·H_2O was derived from the dehydroxylation inside and between cellulose molecular chains and its generation occurred throughout the whole pyrolysis process, which could be confirmed by several small peaks appearing on the FTIR curves. The IR peaks of C=C were similar with H_2O in shape and both of them were distributed on the same position,

Table 3
Kinetic parameters at different heating rates.

Samples	Heating rate (°C/min)	E (kJ/mol)	A (s^{-1})	n	R^2
Un-treated cellulose	10	270.6	$5.33*10^{22}$	0.8	0.995
	20	255.8	$1.50*10^{21}$	1.0	0.990
	40	228.3	$3.70*10^{18}$	0.9	0.998
	80	258.6	$1.46*10^{21}$	1.5	0.983
BM-cellulose	10	187.0	$45.6*10^{14}$	0.2	0.997
	20	179.5	$8.02*10^{14}$	0.4	0.993
	40	166.8	$0.51*10^{14}$	0.3	0.997
	80	182.1	$6.83*10^{14}$	0.5	0.970

Table 2
Thermal characteristic parameters at different heating rates.

Samples	Heating rate (°C/min)	T_i (°C)	T_t (°C)	T_{max} (°C)	D_{max} (°C)	M_r (%)	P (%/°C^2)
Un-treated cellulose	10	310.6	358.3	346.0	2.7	8.4	16.4
	20	325.2	377.3	363.3	2.4	8.8	12.6
	40	338.1	398.3	381.8	2.0	8.5	8.8
	80	346.1	410.6	392.0	1.8	7.5	7.2
BM-cellulose	10	292.9	357.3	337.4	2.6	10.5	11.8
	20	306.6	377.4	353.2	2.3	11.2	9.3
	40	320.6	401.9	372.1	2.1	9.7	7.0
	80	339.8	412.7	393.7	1.8	11.7	6.4

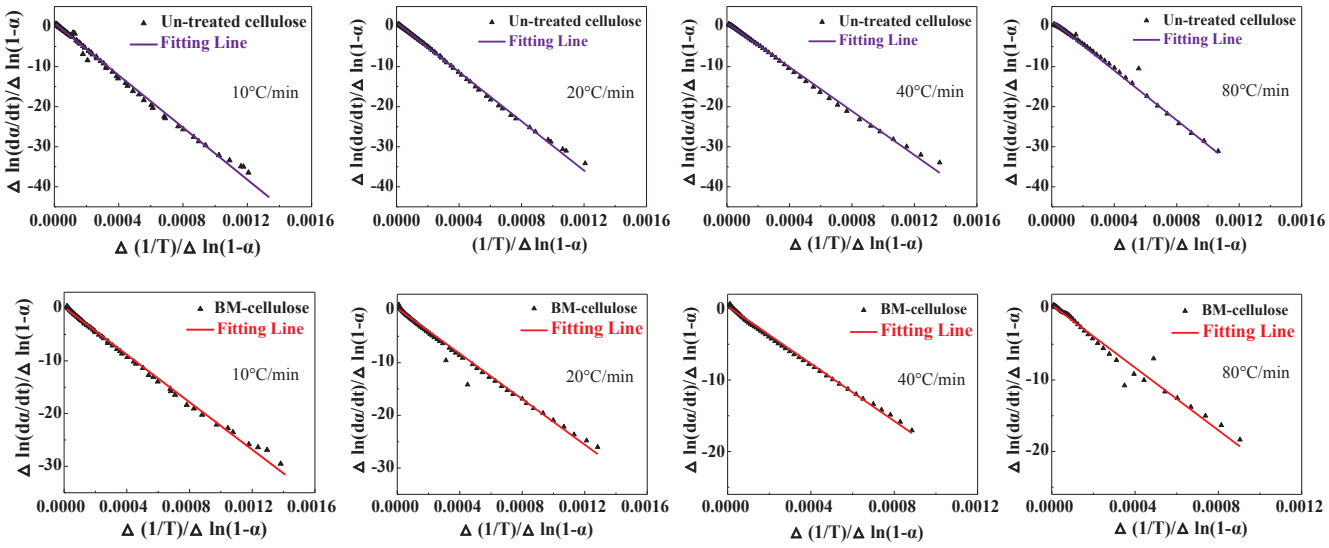

Fig. 4. Fitting straight-lines of Un-treated cellulose and BM-cellulose.

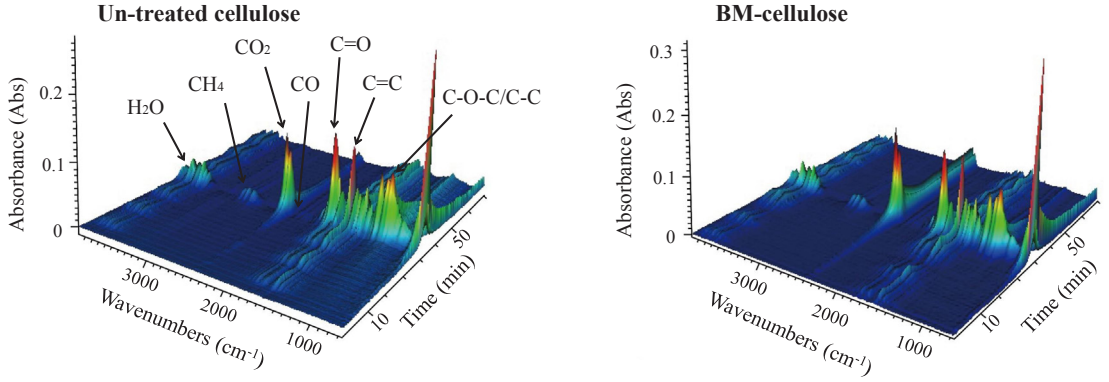

Fig. 5. FTIR three-dimensional spectra of Un-treated cellulose (a) and BM-cellulose (b) during pyrolysis at 10 ˚C/min.

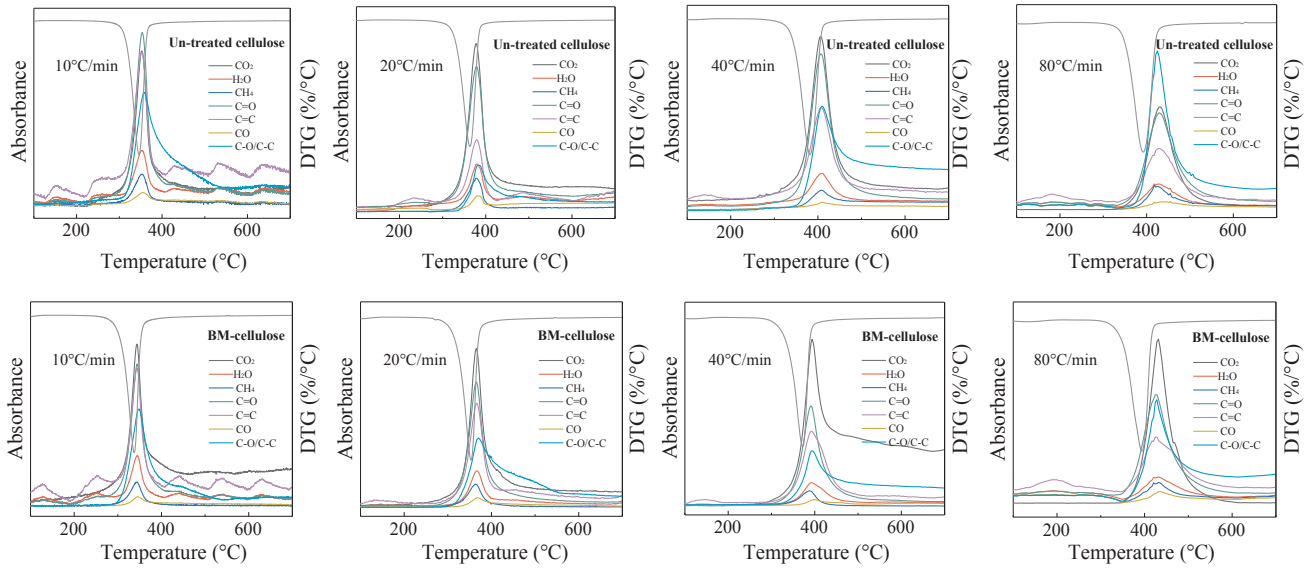

Fig. 6. FTIR profiles of specific functional groups and gaseous products.

thus it could infer that alkenes and aromatics were evolved out from dehydration reaction [31]. But the dehydration reaction was restrained as the heating rate increased. The absorbance intensity of other functional groups in BM-cellulose was similar to that of Un-treated sample. CH_4 mainly derived from the destruction of -O-CH_3- and aliphatic side chains [32]. It could be observed from the absorbance curves that the releasing of C-O-C/C-C lasted for a long time and there was a considerable proportion of C-O-C/C-C releasing at high temperature when

Table 4
Temperature data and absorbance intensity of gaseous products and functional groups.

Samples	Group/Gas	T^a	$I_{max}{}^a$	T^b	$I_{max}{}^b$	T^c	$I_{max}{}^c$	T^d	$I_{max}{}^d$
Un-treated cellulose	CO_2	352.9	0.13	377.3	0.26	406.3	0.38	432.2	0.40
	H_2O	353.4	0.05	379.3	0.08	408.3	0.08	428.5	0.10
	CH_4	353.4	0.03	378.3	0.05	408.3	0.04	424.7	0.10
	C=O	353.4	0.15	378.3	0.23	406.3	0.34	428.5	0.38
	C=C	352.9	0.13	379.3	0.11	408.3	0.23	428.5	0.24
	CO	355.4	0.01	382.4	0.03	410.3	0.02	447.0	0.03
	C-O-C/C-C	358.0	0.10	383.4	0.07	410.3	0.23	424.7	0.62
BM-cellulose	CO_2	343.6	0.17	365.7	0.27	393.7	0.49	431.7	0.61
	H_2O	345.1	0.05	366.7	0.06	391.7	0.07	431.7	0.10
	CH_4	344.1	0.03	363.6	0.04	387.8	0.04	431.7	0.08
	C=O	344.1	0.15	365.7	0.21	391.7	0.29	428.0	0.41
	C=C	344.1	0.14	366.7	0.18	391.7	0.22	428.0	0.25
	CO	346.2	0.01	367.7	0.02	401.6	0.02	435.5	0.05
	C-O-C/C-C	348.2	0.10	370.7	0.12	393.7	0.16	428.0	0.39

I_{max} refers to the maximal absorbance intensity at specific wavenumber;
T refers to the corresponding temperature of I_{max};
[a] the sample heated at 10 °C/min;
[b] the sample heated at 20 °C/min;
[c] the sample heated at 40 °C/min;
[d] the sample heated at 80 °C/min.

cellulose underwent carbonization reaction, which became evident as the heating rate growing up.

4. Conclusion

In this paper, the pyrolysis behavior and kinetic analysis of cellulose with different structures were explored by TG-FTIR and n-order reaction model. BM-pretreatment was applied to decrease the DP and CrI of cellulose, resulting in a decline in thermal stability. The T_i and T_{max} of BM-cellulose were lower than those of Un-treated cellulose in thermogravimetric analyses. The global activation energy and pre-exponential factor of BM-cellulose (166.8–187.0 kJ/mol, 10^{14} s^{-1}) were lower than those of Un-treated cellulose (228.3–270.6 kJ/mol, 10^{20} s^{-1}) in kinetic analyses. TG-FTIR experiment also shown that BM-cellulose yielded more CO_2 and H_2O than Un-treated cellulose. In the future, it would also pay more attention to illustrate the physical structure features and chemical compositions of lignocellulose in sub-micrometer and nanometer levels and their relationship with the formation of value-added products by pyrolysis.

CRediT authorship contribution statement

Fei-xiang Xu: Formal analysis, Writing - original draft. **Xu Zhang:** Formal analysis, Software, Data curation. **Fan Zhang:** Methodology, Data curation, Resources. **Li-qun Jiang:** Supervision, Methodology, Writing - original draft, Validation, Funding acquisition. **Zeng-li Zhao:** Project administration. **Hai-bin Li:** Writing - review & editing.

Declaration of Competing Interest

The authors declare that they have no known competing financial interests or personal relationships that could have appeared to influence the work reported in this paper.

Acknowledgements

Financial support provided by the National Natural Science Foundation of China (No. 51606204), the Project Foundation of Guangdong province and Guangzhou city (No. 2017A020216007 and No. 201707010236), the Open Project of Key State Laboratory of Microbial Technology (No. M2019-10) are gratefully acknowledged.

References

[1] Bilgili F, Koçak E, Bulut Ü, Kuşkaya S. Can biomass energy be an efficient policy tool for sustainable development? Renewable Sustainable Energy Rev 2017;71:830–45.
[2] Wang S, Dai G, Yang H, Luo Z. Lignocellulosic biomass pyrolysis mechanism: a state-of-the-art review. Prog Energy Combust Sci 2017;62:33–86.
[3] Dhyani V, Bhaskar T. A comprehensive review on the pyrolysis of lignocellulosic biomass. Renewable Energy 2018;129:695–716.
[4] Sindhu R, Binod P, Pandey A. Biological pretreatment of lignocellulosic biomass–An overview. Bioresour Technol 2016;199:76–82.
[5] Jiang LQ, Zheng AQ, Meng JG, Wang XB, Zhao ZL, Li HB. A comparative investigation of fast pyrolysis with enzymatic hydrolysis for fermentable sugars production from cellulose. Bioresour Technol 2019;274:281–6.
[6] Shen DK, Gu S. The mechanism for thermal decomposition of cellulose and its main products. Bioresour Technol 2009;100(24):6496–504.
[7] Jiang LQ, Wu YX, Wang XB, Zheng AQ, Zhao ZL, Li HB. Crude glycerol pretreatment for selective saccharification of lignocellulose via fast pyrolysis and enzyme hydrolysis. Energy Convers Manage 2019;199:111894.
[8] Collard FX, Blin J. A review on pyrolysis of biomass constituents: mechanisms and composition of the products obtained from the conversion of cellulose, hemicelluloses and lignin. Renewable Sustainable Energy Rev 2014;38:594–608.
[9] Kan T, Strezov V, Evans TJ. Lignocellulosic biomass pyrolysis: a review of product properties and effects of pyrolysis parameters. Renewable Sustainable Energy Rev 2016;57:1126–40.
[10] Zhang J, Luo J, Tong D, Zhu L, Dong L, Hu C. The dependence of pyrolysis behavior on the crystal state of cellulose. Carbohydr Polym 2010;79(1):164–9.
[11] Mettler MS, Paulsen AD, Vlachos DG, Dauenhauer PJ. The chain length effect in pyrolysis: bridging the gap between glucose and cellulose. Green Chem 2012;14(5):1284–8.
[12] Zhang J, Nolte MW, Shanks BH. Investigation of primary reactions and secondary effects from the pyrolysis of different celluloses. ACS Sustainable Chem Eng 2014;2(12):2820–30.
[13] Jiang LQ, Fang Z, Zhao ZL, Zheng AQ, Wang XB, Li HB. Levoglucosan and its hydrolysates via fast pyrolysis of lignocellulose for microbial biofuels: a state-of-the-art review. Renewable Sustainable Energy Rev 2019;105:215–29.
[14] Li S, Ma X. Catalytic characteristics of the pyrolysis of lignite over oil shale chars. Appl Therm Eng 2016;106:865–74.
[15] Leng E, Costa M, Peng Y, Zhang Y, Gong X, Zheng A, et al. Role of different chain end types in pyrolysis of glucose-based anhydro-sugars and oligosaccharides. Fuel 2018;234:738–45.
[16] Striūgas N, Skvorčinskienė R, Paulauskas R, Zakarauskas K, Vorotinskienė L. Evaluation of straw with absorbed glycerol thermal degradation during pyrolysis and combustion by TG-FTIR and TG-GC/MS. Fuel 2017;204:227–35.
[17] Oudghiri F, Allali N, Quiroga JM, Rodríguez-Barroso MR. TG–FTIR analysis on pyrolysis and combustion of marine sediment. Infrared Phys Technol 2016;78:268–74.
[18] Fang S, Yu Z, Ma X, Lin Y, Lin Y, Chen L, et al. Co-pyrolysis characters between combustible solid waste and paper mill sludge by TG-FTIR and Py-GC/MS. Energy Convers Manage 2017;144:114–22.
[19] Yang X, Zhao Y, Li R, Wu Y, Yang M. A modified kinetic analysis method of cellulose pyrolysis based on TG–FTIR technique. Thermochim Acta 2018;665:20–7.
[20] Janković B, Manić N, Dodevski V, Popović J, Rusmirović JD, Tošić M. Characterization analysis of Poplar fluff pyrolysis products. Multi-component kinetic study. Fuel 2019;238:111–28.
[21] Guo J, Lua AC. Kinetic study on pyrolytic process of oil-palm solid waste using two-

step consecutive reaction model. Biomass Bioenergy 2001;20(3):223–33.
[22] Segal L, Creely JJ, Martin-Jr AE, Conrad CM. An empirical method for estimating the degree of crystallinity of native cellulose using the X-ray diffractometer. Text Res J 1959;29(10):786–94.
[23] Oh SY, Yoo DI, Shin Y, Kim HC, Kim HY, Chung YS, et al. Crystalline structure analysis of cellulose treated with sodium hydroxide and carbon dioxide by means of X-ray diffraction and FTIR spectroscopy. Carbohydr Res 2005;340(15):2376–91.
[24] Wang Z, McDonald AG, Westerhof RJ, Kersten SR, Cuba-Torres CM, Ha S, et al. Effect of cellulose crystallinity on the formation of a liquid intermediate and on product distribution during pyrolysis. J Anal Appl Pyrolysis 2013;100:56–66.
[25] Chen D, Zhou J, Zhang Q. Effects of heating rate on slow pyrolysis behavior, kinetic parameters and products properties of moso bamboo. Bioresour Technol 2014;169:313–9.
[26] Patil SK, Lund CR. Formation and growth of humins via aldol addition and condensation during acid-catalyzed conversion of 5-hydroxymethylfurfural. Energy Fuels 2011;25(10):4745–55.
[27] Wang Z, Pecha B, Westerhof RJ, Kersten SR, Li CZ, McDonald AG, et al. Effect of cellulose crystallinity on solid/liquid phase reactions responsible for the formation of carbonaceous residues during pyrolysis. Ind Eng Chem Res 2014;53(8):2940–55.
[28] Xing S, Yuan H, Qi Y, Lv P, Yuan Z, Chen Y. Characterization of the decomposition behaviors of catalytic pyrolysis of wood using copper and potassium over thermogravimetric and Py-GC/MS analysis. Energy 2016;114:634–46.
[29] Khan AS, Man Z, Bustam MA, Kait CF, Khan MI, Muhammad N, et al. Impact of ball-milling pretreatment on pyrolysis behavior and kinetics of crystalline cellulose. Waste Biomass Valorization 2016;7(3):571–81.
[30] Wang S, Liu Q, Luo Z, Wen L, Cen K. Mechanism study on cellulose pyrolysis using thermogravimetric analysis coupled with infrared spectroscopy. Front Energy Power Eng China 2007;1(4):413–9.
[31] Li S, Lyons-Hart J, Banyasz J, Shafer K. Real-time evolved gas analysis by FTIR method: an experimental study of cellulose pyrolysis. Fuel 2001;80(12):1809–17.
[32] Yang H, Yan R, Chen H, Lee DH, Zheng C. Characteristics of hemicellulose, cellulose and lignin pyrolysis. Fuel 2007;86(12–13):1781–8.